Effects of random fields on the phase transitions and phase diagram of $Mn_{0.75}Zn_{0.25}F_2$

Y. Shapira
Francis Bitter National Magnet Laboratory, Massachusetts Institute of Technology, Cambridge, Massachusetts 02139

N. F. Oliveira, Jr.
Instituto de Fisica, Universidade de São Paulo, Caixa Postal 20516, São Paulo, S.P., 05508, Brazil

S. Foner
Francis Bitter National Magnet Laboratory and Department of Physics, Massachusetts Institute of Technology, Cambridge, Massachusetts 02139

(Received 27 January 1984; revised manuscript received 25 May 1984)

The magnetic phase transitions and phase diagram of $Mn_{0.75}Zn_{0.25}F_2$ are investigated by dilatometric, ultrasonic-attenuation, and magnetization measurements. The random fields, generated by the magnetic field H, affect all three phase boundaries: the spin-flop line $H_{sf}(T)$ separating the antiferromagnetic (AF) phase from the spin-flop (SF) phase; the boundary $T_c^{||}(H)$ between the paramagnetic (P) and AF phases; and the P-SF boundary $T_c^{\perp}(H)$. At $T=0$, $H_{sf}=58.2\pm0.3$ kOe. At high temperatures the boundary $H_{sf}(T)$ is reentrant, in disagreement with the mean-field prediction. Near the P-AF transitions the differential thermal expansion and differential magnetostriction exhibit hysteresis effects when the transition field is above about 12 kOe. In low fields the P-AF transitions are quite sharp, in agreement with earlier data. In high fields the P-AF transitions are smeared if the sample is cooled at constant H or if H is reduced at constant T. The P-AF transitions at high H are sharper if the sample is warmed in a field after it has been cooled in zero field. The hysteretic behavior at high H is consistent with recent theory. The transition temperature $T_c^{||}$ is depressed substantially by the random fields. The crossover exponent obtained from the low-field results for $T_c^{||}$ is $\phi=1.25\pm0.07$, which agrees with the Fishman-Aharony prediction. The Néel temperature is 46.0 K. The P-SF transition temperature $T_c^{\perp}$ increases with increasing H up to 131 kOe. This increase of $T_c^{\perp}$ is much larger than in pure MnF_2, but is consistent with other data in site-random uniaxial antiferromagnets. The phase diagram in the bicritical region is qualitatively different from that in pure MnF_2. Also, we do not observe the two separate critical lines which surround the intermediate phase suggested by Aharony.

I. INTRODUCTION

The drastic effects of random fields on phase transitions and critical behavior have been discussed theoretically since the mid 1970s.[1] Experimental works on this subject were stimulated by Fishman and Aharony.[2] They showed that staggered random fields are generated in random-bond Ising antiferromagnets which are subjected to a uniform magnetic field $\vec{H}$ parallel to the easy axis. The same is also true for site-random antiferromagnets in a field $\vec{H}$.[3] One such site-random system is Zn-doped MnF_2. This system is attractive because MnF_2 is one of the simplest and better-known three-dimensional (3D) easy-axis antiferromagnets. The staggered random fields in Zn-doped MnF_2 are generated by applying a magnetic field parallel to the tetragonal axis, [001].

In earlier papers by our group[4,5] we presented data concerning the phase transitions and phase diagram in $Mn_{1-x}Zn_xF_2$, for $x=0.04$ and 0.125. In the present paper we present and discuss the data for $x=0.25$. Many of the results of the present work are similar to those we obtained earlier, but the effects caused by the random fields are more pronounced here because of the higher Zn concentration. These effects include (1) the reentrant shape of the spin-flop line $H_{sf}(T)$ near the bicritical point, (2) a qualitative change of the phase diagram in the bicritical region, (3) hysteresis effects near the transition from the paramagnetic (P) phase to the antiferromagnetic (AF) phase at finite H, and (4) the depression of the P-AF transition temperature $T_c^{||}$ by the random fields. We also observed a smearing of the P-AF transition at high H when the transition was approached from the paramagnetic side. Finally, we have determined the crossover exponent ϕ which governs the boundary $T_c^{||}(H)$ at low H. A slightly higher value for ϕ in the $(Mn,Zn)F_2$ system was reported by the group at Santa Barbara.[6]

Much of the background material for the present work was already summarized in Ref. 5. Here we cite only more recent works. Many of these relate to the controversy concerning the lower critical dimension d_l for the Ising model in a random field, i.e., whether $d_l=2$ or $d_l\geq3$. For a 3D system, a long-range order cannot exist at a finite temperature T if $d_l\geq3$, but it can exist if $d_l=2$. Theoretical evidence in support of $d_l=2$ was recently summarized by Grinstein.[7] Based on their experimental data the group at Santa Barbara also concluded that $d_l<3$.[8] On the other hand, extensive investigations of several systems by neutron diffraction have led Birgeneau *et al.*[9,10] and Cowley *et al.*[10] to conclude that $d_l\geq3$. According to a recent theoretical work by Villain,[11] $d_l=2$ at

equilibrium, but the finite-time behavior of samples cooled in the presence of a random field corresponds to $d_l=4$.

The dependence of the properties of $Mn_{0.875}Zn_{0.125}F_2$ on the history of the sample (i.e., hysteresis effects in the presence of random fields) was reported in Ref. 5. Hysteresis was also observed in $Mn_{0.78}Zn_{0.22}F_2$ by Cowley and Buyers,[12] and in several other systems.[3,9,10] Such hysteresis effects are consistent with recent theory.[11]

This paper is arranged as follows. The experimental techniques are described in Sec. II. Spin-flop transitions, and the spin-flop line $H_{sf}(T)$, are discussed in Sec. III. Section IV is devoted to hysteresis effects near the P-AF transitions for $H\neq 0$. The P-AF phase boundary, and the crossover exponent ϕ, are discussed in Sec. V. The boundary between the P phase and the spin-flop (SF) phase, and the phase diagram in the bicritical region, are discussed in Sec. VI.

II. EXPERIMENTAL PROCEDURE

Magnetic phase transitions were investigated using dilatometry, ultrasonic attenuation, and magnetization measurements. The dilatometry measurements were of two types: thermal expansion (TE) and magnetostriction (MS). In both, the length l of the sample along the [001] direction was measured with the applied magnetic field $\vec{H}_0$ also parallel to [001]. In the TE experiments, l was measured as a function of T at a fixed H_0. In the MS experiments, the variation of l with H_0 was measured at a fixed T. The ultrasonic attenuation also was measured either as a function of T at a fixed H_0, or as a function of H_0 at a fixed T. Longitudinal sound waves with a frequency of 27 MHz, and a propagation vector along [001], were used. The experimental techniques were for the most part the same as those in Ref. 5. Therefore, only the changes will be mentioned.

A. Samples

Two samples of Zn-doped MnF_2 were cut from opposite sides of a boule which was grown by the Czochralski technique at the Center for Materials Science and Engineering, Massachusetts Institute of Technology (MIT). The samples were rectangular parallelepipeds, with the long dimension parallel to [001]. Sample 1 had dimensions of $3.2\times 5.0\times 6.5$ mm. Sample 2 had dimensions of $3.6\times 3.6\times 6.7$ mm.

The Mn concentration was determined by atomic-absorption analysis. A portion of sample 1 was analyzed in one laboratory, and a portion of sample 2 was analyzed in another.[13] The results were $x=0.256\pm 0.005$ for sample 1 and $x=0.246\pm 0.01$ for sample 2, where x refers to the composition $Mn_{1-x}Zn_xF_2$. Results for the Néel temperatures of the samples indicate that x in sample 2 was actually lower than that in sample 1 by 0.003. Throughout this paper we use $x=0.25$ to describe the composition of either sample.

From the rounding of the low-field P-AF transitions of sample 2, we estimate that the variation Δx of x in this sample was $\Delta x/x\sim 2\times 10^{-3}$, i.e., the Mn concentration was quite uniform. Because the Mn concentration was less uniform in sample 1, all the figures in this paper are for sample 2. The results for sample 1 will be mentioned only briefly; they always agree with those for sample 2. For comparison purposes we also made some measurements on a sample of nominally pure MnF_2.

B. Thermometry

The system for temperature control was the same as in Ref. 5. The temperature was measured by a platinum resistance thermometer (PRT) and/or by a carbon-glass resistance thermometer (CGRT). The most precise temperature measurements were made in the range 37—47 K, which contains the bicritical and Néel points. The CGRT was calibrated in this range against the PRT. The calibration, which was performed *in situ* at $H=0$, was reproducible to within several mK. The magnetoresistance of this CGRT was previously measured in fields up to 190 kOe.[14] All measurements with the CGRT were corrected for this magnetoresistance. The precision of the temperature measurements in the range 37—47 K was estimated to be 5 mK at $H=0$, 15 mK at 80 kOe, and 30 mK at 130 kOe. The absolute accuracy was better than 0.1 K.

The accuracy of the temperature measurements below 37 K depended on T. At 4 K and below, it was 0.1 K. Between 10 and 37 K, the accuracy changed from 0.5 to 0.1 K.

C. Field alignment, magnetization measurements, and demagnetization correction

The dilatometric and ultrasonic measurements were performed in a NbTi superconducting magnet, and also in a high-field Bitter magnet. In these experiments the magnetic field was aligned parallel to [001] to within 0.1°.

Magnetization data were taken only at 4.2 K. A vibrating-sample magnetometer and a NbTi superconducting magnet were used. The field $\vec{H}_0$ was either parallel or perpendicular to [001], within an accuracy of $\pm 2°$ in both cases.

In the present work the difference between the applied magnetic field $\vec{H}_0$ and the internal magnetic field $\vec{H}$ inside the sample was quite small. For example, the demagnetization correction for sample 2 near T_N was only 0.2%. Such demagnetization corrections are included in all plots of the phase diagram in the T-H plane. However, plots of the raw data always show H_0, which is the experimentally measured quantity.

III. SPIN-FLOP TRANSITIONS

A. Magnetostriction

Below 38 K the spin-flop transition (between the AF and SF phases) was accompanied by a jump in the sample's length l. The magnitude of this jump, δl, decreased as T increased. This is illustrated by the results in Fig. 1. At 4.5 K, $\delta l/l=(1.5\pm 0.3)\times 10^{-5}$. The finite jump in l at 4.5 K implies that the transition is of first order (because l is a derivative of the Gibbs potential with

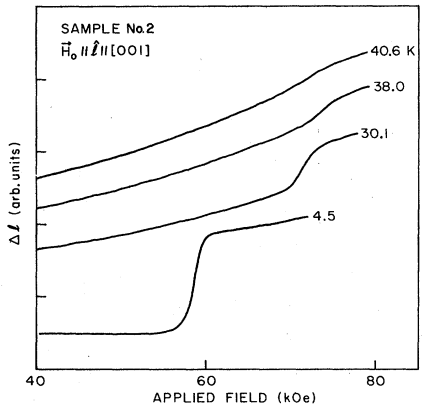

FIG. 1. Traces of the magnetostriction near the spin-flop transitions of $Mn_{0.75}Zn_{0.25}F_2$ at several temperatures. Δl for $\hat{l}||[001]$ is the change in the length of the sample along [001]. $\vec{H}_0$ is the applied magnetic field.

respect to uniaxial pressure). At 38.0 K the transition still appears to be of first order. However, at 40.6 K it is unclear whether the transition is accompanied by a jump in l, or only by an inflection in the MS curve. This will be discussed in Sec. VI C. The data for sample 1 were similar to those in Fig. 1.

The transition field H_{sf} was always chosen at the maximum of $\partial l/\partial(H_0^2)$. This derivative, which was obtained by a numerical differentiation of the raw data, had a spike at low T, and a peak at temperatures near the bicritical point. The choice of H_0^2 as the differentiation variable was made, in part, for consistency with the choice for locating $T_c^{||}$ (Sec. V). We note, however, that had we used the derivative $\partial l/\partial H_0$ to locate H_{sf}, we would have obtained practically the same values, for all T.

B. Magnetization

1. *Results for x = 0.25*

The magnetization of a small portion of sample 2 was measured at 4.2 K. The results are shown in Fig. 2. The curve for $\vec{H}||[001]$ shows the spin-flop transition.[15] It occurs at an internal field $H_{sf}=(58.9\pm0.5)$ kOe, which is in excellent agreement with the MS data. Well above the transition, the susceptibility in the SF phase is $\chi_{SF}=M/H=(3.15\pm0.1)\times10^{-4}$ emu/g. No hysteresis was observed in the magnetization at 4.2 K.

Also shown in Fig. 2 is the low-H portion of the magnetization curve for $\vec{H}\perp[001]$. The high-H portion of this curve was deleted to avoid confusion with the curve for $\vec{H}||[001]$. The two curves are very close to each other above 67 kOe, as expected for a low-anisotropy antiferromagnet.[16] The low-field susceptibility for $\vec{H}\perp[001]$ is $\chi_\perp(0)=(3.29\pm0.1)\times10^{-4}$ emu/g, which corresponds to 3.14×10^{-2} cm^3/mol. At the highest fields the perpendicular susceptibility is slightly smaller, which is expected for $x\neq0$.[17]

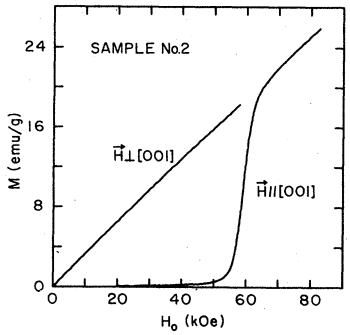

FIG. 2. Traces of the magnetic moment per gram, M, vs H_0 for $Mn_{0.75}Zn_{0.25}F_2$. These results are for sample 2 at 4.2 K.

2. *Results for pure MnF_2*

For comparison purposes the magnetization of a nominally pure sample of MnF_2 was measured at 4.2 K, with $\vec{H}$ parallel and perpendicular to [001]. The results were qualitatively similar to those in Fig. 2. For $\vec{H}\perp[001]$ the susceptibility $\chi_\perp=M/H$ remained constant to better than 2% in fields up to 80 kOe. Its value was $\chi_\perp=(2.72\pm0.06)\times10^{-4}$ emu/g, corresponding to 2.53×10^{-2} cm^3/mol. This result is in good agreement with the value obtained by Trapp and Stout,[18] but is slightly higher than values obtained by Foner[19] and by Gäfvert *et al.*[20]

The data for $\vec{H}||[001]$ were taken in fields up to 110 kOe. The spin-flop field, after a demagnetization correction, was $H_{sf}(4.2\text{K})=(91.5\pm0.5)$ kOe. This value is 1% lower than those obtained in Refs. 21 and 22. From Ref. 22 we expect that H_{sf} at $T=0$ is lower than that at 4.2 K by less than 0.1 kOe. From the magnetization data between 100 and 110 kOe, $\chi_{SF}=M/H=(2.74\pm0.06)\times10^{-4}$ emu/g.

C. Ultrasonic attenuation

The ultrasonic attenuation near the spin-flop transition was studied only in sample 1. Traces of the attenuation versus H were taken at fixed temperatures between 4.2 K and the bicritical point. The spin-flop transition was accompanied by a spike in the attenuation. The height of the spike decreased as T increased. The data were qualitatively similar to those obtained in our previous study[5] for $x=0.125$. The transition field $H_{sf}(T)$, chosen at the attenuation maximum, agreed with the MS results.

D. Phase boundary $H_{sf}(T)$

1. *Reentrant behavior*

The spin-flop boundary $H_{sf}(T)$, separating the AF and SF phases of sample 2, is presented in Fig. 3. Portions of the P-AF and P-SF boundaries are also shown. In contrast to pure MnF_2, for which $H_{sf}(T)$ increases monotonically with increasing T (Ref. 23), the spin-flop line in Fig. 3 bends downward as T increases beyond 38 K. This reentrant behavior of the spin-flop line was also observed

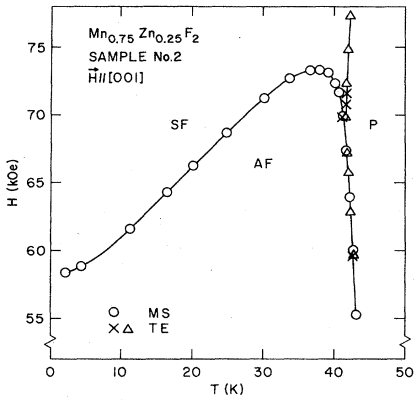

FIG. 3. Spin-flop phase boundary $H_{sf}(T)$, which separates the AF phase from the SF phase. Also shown are portions of the P-AF and P-SF phase boundaries. These data are from magnetostriction (MS) and thermal-expansion (TE) data. H is the internal magnetic field.

in our earlier studies on samples with lower x.[4,5] The boundary $H_{sf}(T)$ for sample 1 agrees with the results in Fig. 3.

The phase diagram of Zn-doped MnF_2 was calculated using the mean-field virtual-crystal approximation.[24] This treatment neglects random fields. It predicts that the boundary $H_{sf}(T)$ in a Zn-doped sample is the same as in pure MnF_2, except that both H and T are scaled by a factor $1-x$. Clearly this prediction does not agree with the reentrant feature which is observed. We believe that this feature is caused by the random fields. (See note added in proof.)

2. *Zero-temperature value of H_{sf}*

Extrapolation of the results in Fig. 3 to $T=0$ gives $H_{sf}(0)=(58.2\pm0.3)$ kOe for $x=0.25$. The mean-field (MF) treatment in Ref. 24 predicts that $H_{sf}(0)$ is proportional to $1-x$, which gives $H_{sf}^{MF}(0)=68.6$ kOe for $x=0.25$. This is 18% above the observed value. For $x=0.125$ the difference between the MF and observed values of $H_{sf}(0)$ is 4% (Ref. 5).

The fact that $H_{sf}(0)$ in Zn-doped MnF_2 is lower than the MF prediction has been known for some time, and it has been discussed extensively in the literature.[25] Here we only point out the existence of an analogy between the spin flop in a diluted low-anisotropy antiferromagnet and the spin flop of a uniaxial ferromagnet which is in a random field.[26] As described in Ref. 5, some of the difference between $H_{sf}(0)$ and $H_{sf}^{MF}(0)$ may be viewed as a consequence of local fluctuations in the orientation of the sublattice magnetization in the SF phase. These fluctuations, which are neglected in MF theory, lower the free energy of the SF phase, thus lowering $H_{sf}(0)$. This mechanism of lowering $H_{sf}(0)$ in a diluted antiferromagnet is analogous to the one which causes a spin flop in a uniaxial ferromagnet which is a random field and at $T=0$. In the case of the ferromagnet, a random field which is parallel to the easy axis produces fluctuations in the orientation of the magnetization in the SF phase.[26] This lowers the free energy of the SF phase, and leads to a spin flop. An analysis of the present results for $x=0.25$ indicates that local fluctuations of the spin orientations in the SF phase cause a 10% reduction of $H_{sf}(0)$ relative to the MF value. The remaining 8% reduction is probably attributable to a lower anisotropy than that given by MF theory, as discussed by Brady Moreira and Fittipaldi.[25]

IV. HYSTERESIS NEAR THE P-AF TRANSITION

The P-AF transition was investigated only by dilatometry. The shapes of the critical anomalies in the differential magnetostriction, $\partial l/\partial H_0$, and the differential thermal expansion, $\partial l/\partial T$, were found to depend on the history of the sample. This hysteretic behavior was already noted in our previous work[5] on $x=0.125$. In the present work the hysteresis was studied more systematically, and was interpreted in terms of a recent theory.[11]

A. Magnetostriction

MS data were obtained as follows. The sample was warmed at zero field to some fixed temperature. A trace of the isothermal MS was then taken as a function of increasing H_0. This trace, called the virgin trace, was stopped at a field well above the AF→P transition. A second trace, which we call MS↓, was then taken in a decreasing H_0. It was stopped well below the transition. A third trace, called MS↑, was then taken as a function of increasing H_0. This was followed by several pairs of MS↓ and MS↑ traces at the same temperature. The field was then reduced to zero and the sample was warmed to a new temperature, typically 0.5 K higher. The procedure was then repeated. A typical sweep rate during any of the MS traces was 4 kOe/min.

Figure 4 shows an example of MS↓ and MS↑ traces at the same temperature. It is obvious that the MS is not reversible. At the transition, which occurs at 21 kOe, the derivative $\partial l/\partial H_0$ for MS↑ is larger than for MS↓. Hysteresis effects in the magnetostriction were observed at all temperatures for which the P-AF transition was above about 12 kOe. For lower transition fields no hysteresis was detected.

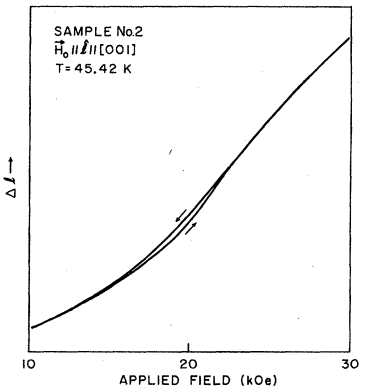

FIG. 4. Traces of the magnetostriction near a P-AF transition, for decreasing and for increasing H_0 (MS↓ and MS↑). Note the hysteresis.

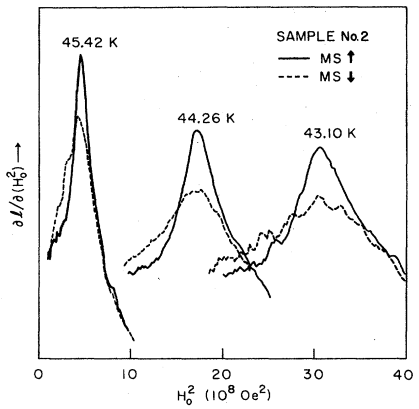

FIG. 5. Traces of the derivative $\partial l/\partial(H_0^2)$, obtained by a numerical differentiation of data for l vs H_0^2. The solid curves are from MS↑ data (increasing H_0), and the dashed curves are from MS↓ data (decreasing H_0) at the same temperatures.

Because H^2 is the scaling variable in the random-field problem,[2] we use it (rather than H) in the analysis of the MS data. Figure 5 shows the results for $\partial l/\partial(H_0^2)$ versus H_0^2 for MS↑ and MS↓ traces at three temperatures. Note that the transitions are sharper for the MS↑ traces. In addition, for both the MS↑ and the MS↓ traces the anomaly in $\partial l/\partial(H_0^2)$ becomes broader and smaller as the transition field increases.

We now discuss the virgin trace, taken during the initial increase of H_0. For temperatures where the transition field was below approximately 40 kOe, the virgin trace was practically indistinguishable from the MS↑ trace. When the transition field was above ~40 kOe the peak in the derivative $\partial l/\partial(H_0^2)$ for the virgin trace was larger than that for the MS↑ trace at the same temperature. This difference increased as the transition field increased.

B. Thermal expansion

Three different procedures were used to collect TE data. In the first, data were taken as the sample cooled at constant H_0, from the P phase to the AF phase. The cooling rate was approximately 50 mK/min. This type of data will be called TE↓. In the second procedure the sample was first cooled at constant H_0 to a temperature approximately 1 K below the transition. The TE data were then taken as the sample was warmed at the same H_0. The cooling and warming rates were both ~50 mK/min. Such data (i.e., warming after cooling in a field) will be called TE↑FC. In the third procedure the sample was first cooled at zero field from a temperature above the Néel temperature T_N to a temperature which was ~1 K below the transition temperature for some field. The field was then applied, and the TE was measured as the sample was warmed at constant H_0. The cooling at zero field was rapid (1 to 10 K/min), but the warming rate was ~50 mK/min. This type of data (warming after cooling in zero field) will be called TE↑ZC.

Figure 6 shows results for the differential thermal expansion, $\partial l/\partial T$, obtained with the three procedures at several fixed fields. (The trace for TE↑FC at 59.7 kOe is not included because it was obtained in another run. This trace is shown in Fig. 7.) As Fig. 6 indicates, the zero-field results for cooling and warming are very similar. However, at finite H_0 the results for $\partial l/\partial T$ depend on the procedure. The sharpest peaks in $\partial l/\partial T$ are observed for warming after cooling in zero field (top row). The peaks observed when the sample is cooled at constant H_0 (bottom row) are smaller and broader, particularly at high H_0. The results for TE↑FC (middle row) are intermediate between these two extremes.

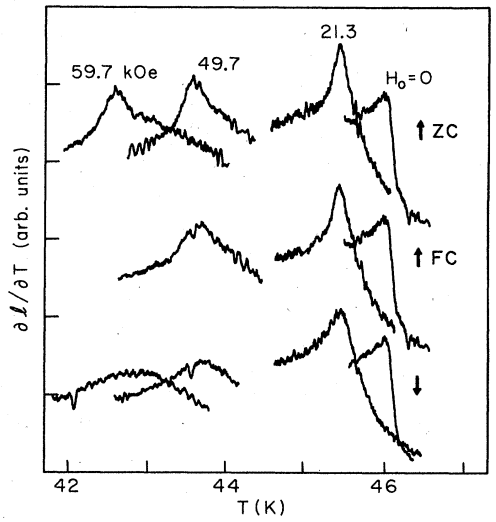

FIG. 6. Differential thermal expansion, $\partial l/\partial T$, near the P-AF transitions at four fixed values of H_0. Upper row is from TE↑ZC data, i.e, warming after cooling in zero field. Middle row is from TE↑FC data, i.e., warming after cooling in the same field. Lower row is from TE↓ data, i.e., cooling. The three rows have been displaced vertically relative to each other. The vertical gain for all traces is the same. The trace for TE↑FC at 59.7 kOe is missing.

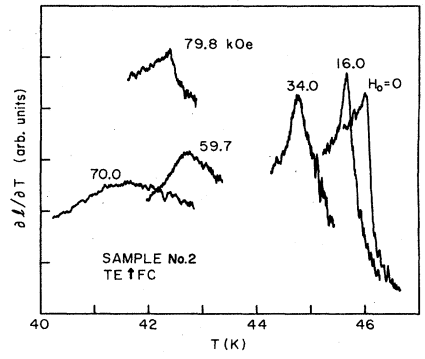

FIG. 7. Differential thermal expansion at six values of H_0. These results are from TE↑FC data. The curve for 79.8 kOe was shifted upward to avoid confusion with other curves. The curves for the lowest four fields show P-AF transitions. The curve at 70 kOe shows a transition in the bicritical region. Its location is consistent with a P-SF transition. The curve at 79.8 kOe shows a P-SF transition well above the bicritical region.

C. Discussion

We first compare our data to those obtained by others on site-random 3D Ising antiferromagnets. As Fig. 6 indicates, the peak in $\partial l/\partial T$ at 21.3 kOe is larger in magnitude and is more symmetric than that at $H_0=0$. This is true for all three procedures of crossing the phase boundary. The peaks obtained with the two warming procedures (↑FC and ↑ZC) also appear to be sharper than the peak at $H_0=0$. These results for 21.3 kOe are qualitatively similar to the low-field birefringence data of Belanger *et al.*[6] in Zn-doped MnF_2 and Zn-doped FeF_2. However, these workers did not report any hysteresis. According to Belanger *et al.*, near the transition the differential birefringence is proportional to the magnetic specific heat C_m. If thermodynamic equilibrium is assumed then the differential thermal expansion, $\partial l/\partial T$, near a second-order transition also is expected to mimic the specific heat.[27] Thus, in the absence of irreversibility the birefringence and TE results should resemble each other. When hysteresis is present, this similarity may not hold. Nevertheless, because the hysteresis which we observed at fields $H_0 \lesssim 21$ kOe was relatively small, the qualitative similarity between the TE and birefringence results at low fields is not surprising. Belanger *et al.*[8] interpreted their results in terms of a random-field-induced change of the effective dimensionality from 3 to 2.

The work of Belanger *et al.* on Zn-doped MnF_2 was carried out only in fields up to 20 kOe. One of the important results of the present work is that the peaks of $\partial l/\partial T$ *when the sample is cooled at constant* H_0 (bottom row in Fig. 6) become smaller and broader at higher fields. Thus, the transition, if it is approached from the paramagnetic side, is smeared by a large random field. This conclusion also agrees with the MS↓ results in Fig. 5, which show that the P→AF transition broadens as the transition field increases. A similar result was obtained in neutron-diffraction studies on several site-random 3D antiferromagnets. The neutron data indicate that the correlation length at the P-AF "transition" is finite when the samples are cooled in a high magnetic field.[10]

The controversy concerning the lower critical dimension d_l (i.e., whether $d_l<3$ or $d_l\geq 3$) was mentioned in Sec. I. Very recent theoretical works[11] suggest that at equilibrium $d_l=2$, but that when a 3D sample is cooled in the presence of a random field, a metastable domain phase (with no long-range order) is established. The domain phase does not transform into the equilibrium phase at finite times. This model agrees with those results[6–8] which give $d_l=2$, but it also explains why data obtained by cooling in a field gave $d_l\geq 3$.[9,10] As emphasized by Birgeneau *et al.*,[10] in many physical realizations of random fields in nature the random fields cannot be removed, unlike the situation in Fishman-Aharony antiferromagnets where there is no random field at $H=0$. When a system in which the random field is always present is cooled, its behavior should be similar to that of a Fishman-Aharony antiferromagnet which is cooled in a field.

The prediction[11] that long-range order is not established at finite times when a 3D diluted antiferromagnet is cooled in a field is consistent with our TE↓ data. The broad anomalies observed when cooling in the presence of high fields are then interpreted as pseudotransitions into a metastable domain phase. Metastable domains at $T<T_c^{\parallel}$ can also account for the hysteresis phenomena which we and others have observed.

Consider Fig. 6. At 59.7 kOe the peak for TE↑ZC (top row) is much sharper than for TE↓ (bottom row), and it also occurs at a slightly lower temperature. Following Ref. 11 we interpret the broad peak for TE↓ as a pseudotransition into a domain phase. This is consistent with recent neutron-diffraction data.[28] These neutron data also indicate that the TE↑ZC procedure (sample is first cooled at $H=0$) leads to (1) long-range order below $T_c^{\parallel}$, and (2) an abrupt collapse of the Bragg peak on warming in a field. The latter result explains why the peak of $\partial l/\partial T$ observed in the TE↑ZC procedure is relatively sharp.

The sample's length l in the AF phase depends on the history of the sample. The raw data for l versus T, corresponding to the results in Fig. 6 for $H_0>0$, indicate that the shortest length at a point in the AF phase is obtained by cooling in zero field and then applying a field. Because the development of antiferromagnetic order leads to a contraction of the sample, this result suggests that the antiferromagnetic order is more fully developed when the sample is first cooled in zero field. A more direct evidence for this conclusion comes from recent neutron-diffraction data.[28]

V. P-AF PHASE BOUNDARY

A. Experimental results

The boundary $T_c^{\parallel}(H^2)$ between the P and AF phases was determined from the TE and MS data. The criteria which were used to locate $T_c^{\parallel}(H^2)$ were the maximum in $\partial l/\partial T$ when the TE was measured, and the maximum in $\partial l/\partial(H_0^2)$ when the MS was measured. The question of whether these maxima correspond to genuine order-disorder transitions or to pseudotransitions was not addressed here.

The P-AF boundary for sample 2 is shown in Fig. 8. Different symbols are used for data points obtained from MS↑, MS↓, TE↓, TE↑FC, and TE↑ZC. (This was not done in Fig. 3, which has a much coarser temperature scale. In that figure the data points are averages for MS↑ and MS↓, averages for TE↓ and TE↑FC, and TE↑ZC.) Also shown in Fig. 8 are portions of the P-SF boundary $T_c^{\perp}(H^2)$ and the spin-flop line $H_{sf}^2(T)$. The Néel temperature of sample 2 is $T_N=(46.00\pm 0.02)$ K, where the 0.1-K uncertainty in the calibration of the reference platinum thermometer is not included. The Néel temperature of sample 1 is 0.2 K lower than that for sample 2.

The two interesting regions in Fig. 8 are the bicritical region and the low-field region. The low-H region is considered next. The bicritical region is discussed in Sec. VI.

B. Low-field results and the crossover exponent ϕ

In a pure easy-axis antiferromagnet such as MnF_2 the transition temperature $T_c^{\parallel}$ decreases linearly with H^2 at

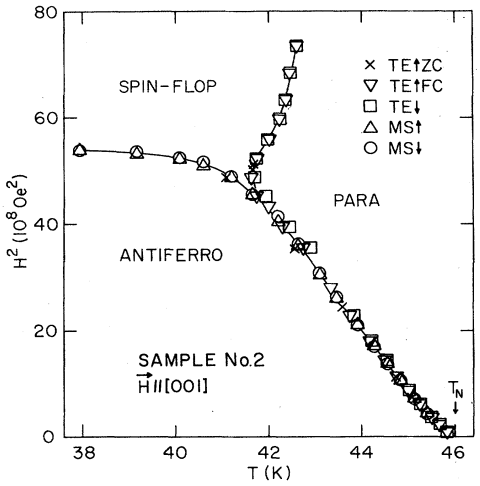

FIG. 8. Phase diagram of sample 2, between 38 K and the Néel temperature, $T_N=(46.00\pm0.02)$ K. Different symbols for the data points correspond to results obtained with different procedures (TE↑ZC, TE↑FC, TE↓, MS↑, and MS↓). Some data points were suppressed to avoid overcrowding. The lines are merely guides to the eye.

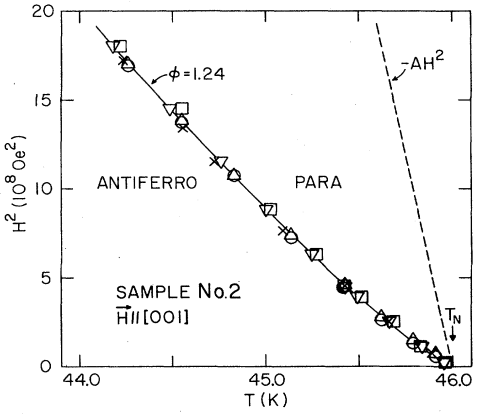

FIG. 9. Low-field portion of the P-AF phase boundary. All data points in this field range are included. The symbols for the data points are as in Fig. 8. The dashed straight line, $-AH^2$, is the estimated phase boundary in the absence of random fields. The solid curve is a best fit to Eq. (1), with A held fixed at 2.09×10^{-10} K/Oe^2, and with T_N held fixed at 46.00 K. This fit gives $\phi=1.24$. Other fits are discussed in the text.

low fields.[23] On the other hand, for a random antiferromagnet in a magnetic field parallel to the easy axis, $T_c^{||}$ should be given by[2]

$$T_c^{||}-T_N=-AH^2-BH^{2/\phi}\ , \tag{1}$$

where A and B are constants, and ϕ is a crossover exponent which is predicted to be equal to the (staggered) susceptibility exponent γ at $H=0$. Strictly, this γ is for the Ising model with random-exchange interactions. Its theoretical value is $\gamma=1.39$ (Ref. 29) or 1.34 (Ref. 30). However, because the crossover from pure Ising to random-exchange Ising behavior is very slow, Fishman and Aharony[2] predicted that the observed effective ϕ would be close to γ for the pure Ising model, i.e., $\gamma=1.25$. Some recent results[8] for ϕ agree with a random-exchange γ, while others[3] agree with a pure Ising γ.

The term $BH^{2/\phi}$ should lead to a curvature in a plot of $T_c^{||}$ versus H^2. This prediction is verified by the low-field data in Fig. 9. In this figure the dashed line is an estimate of the term $-AH^2$. It was obtained by using the MF result[24]

$$A(x)/A(0)=(1-x)^{-1}$$

for $Mn_{1-x}Zn_xF_2$ and $A(0)=1.57\times10^{-10}$ K/Oe^2 (Ref. 23). That is, $A(x=0.25)=2.09\times10^{-10}$ K/Oe^2. It is obvious from Fig. 9 that the random-field-term $-BH^{2/\phi}$ gives the dominant contribution to the depression of $T_c^{||}$ with increasing H.

To obtain the crossover exponent ϕ, the data for $T_c^{||}$ were fitted to Eq. (1). In principle, it should have been possible to obtain all the parameters in Eq. (1) from the fit to the data. However, in practice, the accuracy of the data was such that meaningful results were not obtained when A was allowed to vary, i.e., too many adjustable parameters. We therefore estimated A and held it fixed. This procedure was also used in all earlier experimental determinations of ϕ.[3,5,6,8] As already mentioned, we estimated A by using the MF result

$$A(x)/A(0)=(1-x)^{-1}$$

and the known $A(0)$. This estimate suffers from the drawback of being based on a MF treatment[24] which neglects random fields. In principle, the random field may give rise to an analytical contribution to $T_c^{||}$, in addition to the singular contribution $-BH^{2/\phi}$ in Eq. (1). The analytical contribution is, to lowest order, proportional to H^2, so that it can affect A. All our results for ϕ will be based on the assumption that the random-field correction for A is small. It will be shown that a 10% change in A has only a minor effect on ϕ. However, the possibility of a larger error in A cannot be ruled out. All the earlier experimental results for ϕ (Refs. 3, 5, 6, and 8) suffer from a similar difficulty.

Various fits of data to Eq. (1) were made for the purpose of obtaining the crossover exponent ϕ. In one fit all 42 data points in Fig. 9 (for $H^2\le18\times10^8$ Oe^2) were used, T_N was held fixed at its measured value 46.00 K, A was held fixed at 2.09×10^{-10} K/Oe^2, and B and ϕ were treated as adjustable parameters. This fit, which gave $\phi=1.24\pm0.01$, is shown as a solid curve in Fig. 9. A similar fit, but with T_N treated as an adjustable parameter, gave $\phi=1.28\pm0.03$ and $T_N=(46.02\pm0.01)$ K. This value for T_N is still consistent with $T_N=(46.00\pm0.02)$ K obtained from the TE data at $H=0$.

We have also repeated the fits with a slightly different value of A, based on an alternative estimate[3]

$$A(x)/A(0)=T_N(0)/T_N(x)=2.30\times10^{-10}\ \text{K/Oe}^2\ .$$

This gave $\phi=1.25\pm0.01$ for a fixed T_N and $\phi=1.29\pm0.03$ for an adjustable T_N. Thus, ϕ is not sensitive to a 10% change of A. To obtain some idea of the ef-

fect of a large change in A, we also made fits with $A=0$. These gave $\phi=1.19$ for fixed T_N and $\phi=1.22$ for an adjustable T_N. Finally, we made fits with $A=4.18\times10^{-10}$ K/Oe^2 (i.e., twice the original estimate). These gave $\phi=1.33$ and 1.42 for fixed and adjustable T_N, respectively. All the remaining fits described below are with the original estimate, $A=2.09\times10^{-10}$ K/Oe^2.

In addition to the fits to all the data points, separate fits were made to the data for MS↑, MS↓, TE↓, TE↑FC, and TE↑ZC. With T_N fixed, the fits gave ϕ's between 1.23 and 1.27. For an adjustable T_N the ϕ's were between 1.26 and 1.32.

Equation (1) is expected to hold only at low fields. We therefore examined the dependence of ϕ on the range of H^2. For this purpose, separate fits were performed for different ranges. In each fit all data points in the range $0<H^2\leq H^2_{\max}$ were used. The results when T_N was held fixed are shown in Fig. 10(a). They suggest a slight systematic decrease of ϕ with decreasing $H^2_{\max}$. This trend may have been caused by a slightly too low value for T_N. The value which we used corresponded to the maximum in the differential-thermal-expansion anomaly at $H=0$. Owing to the rounding and asymmetry of this anomaly, the actual value for T_N may be slightly higher (see Sec. IV B 1 of Ref. 5). The effects of this error on the results for ϕ should increase as $H^2_{\max}$ decreases. The results for ϕ when T_N was treated as an adjustable parameter are shown in Fig. 10(b). The fits which led to Fig. 10(b) also gave values for T_N. These were all in the range 46.01 to 46.035 K [compared with $T_N=(46.00\pm0.02)$ K from the TE data at $H=0$].

Finally, we have also fitted the data for sample 1 (in the range $0<H^2<18\times10^8$ Oe^2) to Eq. (1). Here, again, A was held fixed at 2.09×10^{-10} K/Oe^2. We obtained $\phi=1.21\pm0.01$ for a fixed T_N and 1.26 ± 0.03 for an adjustable T_N.

Based on our results for both samples, we estimate that $\phi=1.25\pm0.07$. This agrees with γ for the pure Ising model, as originally predicted by Fishman and Aharony.[2] Our value is barely consistent with $\phi=1.4\pm0.1$ obtained by Belanger *et al.*[6] in $Mn_{1-x}Zn_xF_2$, but is lower than their value $\phi=1.40\pm0.05$ for $Fe_{0.6}Zn_{0.4}F_2$ (Ref. 8). The discrepancy between the result in $Fe_{0.6}Zn_{0.4}F_2$ and our value is not necessarily significant; in one system the effective ϕ may be close to γ for the random-exchange model, while in another it may be close to γ for the pure Ising model. Our result for ϕ is in good agreement with that obtained by Wong *et al.* in $Fe_{1-x}Mg_xCl_2$.[3] Finally, we note that lower values for ϕ were obtained in our previous works on samples with lower x.[4,5] These lower values were attributed to the unfavorable ratio between $BH^{2/\phi}$ and AH^2 in low-concentration samples. In the present work this ratio is more favorable (Fig. 9).

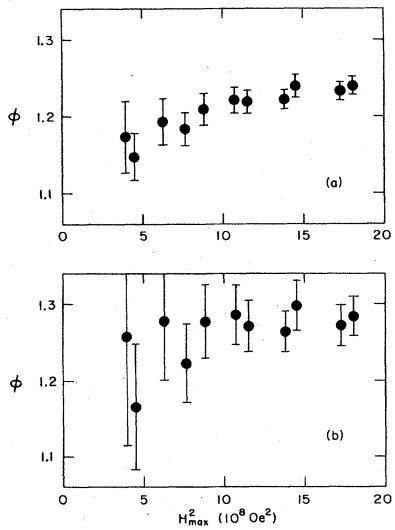

FIG. 10. Crossover exponent ϕ, obtained from fits of the data in sample 2 to Eq. (1). Each fit is for all data points in the range $0<H^2\leq H^2_{\max}$. The parameter A is held fixed at 2.09×10^{-10} K/Oe.[2] (a) Results with T_N held fixed at 46.00 K. (b) Results with T_N treated as an adjustable parameter. The error bars are $\pm\sigma_\phi$, where σ_ϕ is one standard deviation.

VI. P-SF PHASE BOUNDARY AND THE BICRITICAL REGION

A. P-SF transitions

The P-SF transitions in sample 2 were observed in TE measurements carried out in fields up to 86 kOe. Most of the data were of the TE↓ and TE↑FC types. For these two types of data the critical anomalies had similar shapes at all fields, and they also occurred at the same temperature, $T_c^\perp(H)$, i.e., no hysteresis.

Three TE↑ZC traces were taken between 70 and 72 kOe, which is in the bicritical region (see Figs. 3 and 8). At 71.7 kOe the anomaly in $\partial l/\partial T$ had a similar shape to those obtained from TE↓ and TE↑FC data at 72.4 kOe. However, the derivative of the TE↑ZC trace at 70 kOe had a peak at the AF-SF transition (at a temperature below $T_c^\perp$), whereas the TE↓ and TE↑FC data at the same field only showed the P-SF transition at $T_c^\perp$. At 71 kOe the derivative of the TE↑ZC trace had both a peak at $T_c^\perp$ and a "shoulder" at the AF-SF transition.

In summary, there is no hysteresis in fields above the bicritical region (i.e., $H>72$ kOe), but there is a hysteresis near 70 kOe. The absence of hysteresis in fields above the bicritical region is expected because the random field is parallel to [001], and it does not couple to the order parameter of the SF phase, which is perpendicular to [001]. Our data for $x=0.125$ led to a similar conclusion.[5]

For fields above 75 kOe the critical anomaly in $\partial l/\partial T$ was relatively sharp. This is illustrated in Fig. 7 by the result for 79.8 kOe. As H decreased below 75 kOe, the critical anomaly became broader. These results are consistent with recent neutron-diffraction data which show that long-range order is established only above 75 kOe.[28]

TE data were also taken on sample 1. They were all of the TE↓ and TE↑FC types. The results near the P-SF transitions were similar to those for sample 2. The P-SF transitions in sample 1 were also observed in ultrasonic-attenuation measurements between 76 and 131 kOe. The

transition appeared as a peak in the attenuation versus T at constant H_0.

B. P-SF phase boundary

The P-SF transition temperature $T_c^{\perp}(H^2)$ was chosen at the maximum of $\partial l/\partial T$, or at the maximum of the ultrasonic attenuation versus T. For sample 1 there was good agreement between the TE and ultrasonic results in the field range where both data were taken. The P-SF phase boundary in sample 2 is shown in Fig. 8. These data indicate that $T_c^{\perp}$ increases with increasing H in fields up to 86 kOe. The data for $T_c^{\perp}$ in sample 1 were similar, except for a shift of 0.2 K to lower temperatures, which corresponds to the lower T_N in this sample. The ultrasonic data in sample 1 showed that $T_c^{\perp}$ continues to increase with increasing H at least up to 131 kOe ($H^2=172\times10^8$ Oe^2). From the results for $x=0.04$ (Ref. 4), we expect that at somewhat higher fields $T_c^{\perp}$ starts to decrease with increasing H.

The increase of $T_c^{\perp}$ between 71 and 86 kOe is 0.9 K. The data for sample 1 show that an additional increase of 0.5 K occurs between 86 and 131 kOe. The total increase of $T_c^{\perp}$ between 71 and 131 kOe is more than an order of magnitude larger than the corresponding increase in pure MnF_2.[23] Qualitatively similar results were obtained earlier in the samples with $x=0.04$ and 0.125,[4,5] and also in La- and Bi-doped $GdAlO_3$.[31] The much larger increase of $T_c^{\perp}$ in Zn-doped MnF_2, compared to pure MnF_2, presumably is caused by the random fields.

The precise location of the bicritical point was not determined in the present work because of the hysteresis and the broad transitions in the bicritical region.

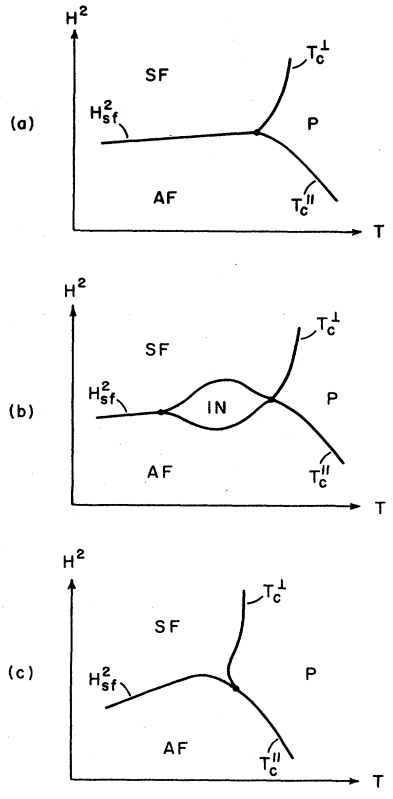

FIG. 11. Sketches of several phase diagrams in the bicritical region. (a) The usual phase diagram for a pure easy-axis antiferromagnet. (b) A phase diagram suggested by Aharony, when random fields are present. (c) A phase diagram suggested by our experimental results.

C. Discussion of the bicritical region

Recent neutron-diffraction data[28] suggest that the behavior in the bicritical region is more complicated than one might be led to believe on the basis of Figs. 3 and 8. Specifically, there is no long-range order in the region of the SF phase which is near the bicritical point in Fig. 3 (see note added in proof). No detailed theoretical explanation of this behavior is available at present. In what follows we compare our phase diagram with predictions for a pure antiferromagnet, and with early predictions for the behavior in the presence of a random field.

The usual phase diagram near the bicritical point of a pure easy-axis antiferromagnet[32] is shown schematically in Fig. 11(a). This figure describes the behavior of pure MnF_2.[23,33] However, the experimental results in Figs. 3 and 8 indicate that the phase diagram for $x=0.25$ is qualitatively different. In particular, the spin-flop line for $x=0.25$ has a reentrant portion, unlike the line in pure MnF_2.[23] Because Fig. 11(a) does not seem to apply here, we believe that the lines $T_c^{\parallel}$ and $T_c^{\perp}$ in the bicritical region should not be fitted in the manner described by Rohrer.[31] In his fit, the only change in the standard expression for a pure antiferromagnet[32] is the use of two *different* shift exponents for the lines $T_c^{\parallel}$ and $T_c^{\perp}$.

A different type of phase diagram was proposed by Aharony.[34] It is shown in Fig. 11(b). Here, the spin-flop line $H_{sf}^2(T)$ splits into two second-order lines which enclose an intermediate phase (IN). These two lines reunite at a higher temperature, where they meet the lines $T_c^{\parallel}$ and $T_c^{\perp}$. The point where all four lines meet is then a tetracritical point. To make Fig. 11(b) consistent with our data we must assume that the spin-flop line in Fig. 3 is actually composed of two lines in Fig. 11(b), namely the spin-flop line and the upper of the two lines which surround the IN phase. This would then explain the reentrant feature of the spin-flop line. Furthermore, the spin-flop transitions which we observed at $T\gtrsim40$ K might have been of second order (Sec. III A), which is consistent with Fig. 11(b). On the other hand, several features of our data do not seem to agree with Fig. 11(b). First, we did not observe any anomalies which could be associated with the lower of the two lines surrounding the IN phase in Fig. 11(b). Second, the lower portion of the line $T_c^{\perp}$ in Fig. 8 does not seem to agree with Fig. 11 (b). Finally, the spin-flop transitions for temperatures up to 38 K (where H_{sf} is maximum) appear to be of first order, whereas Fig. 11(b) indicates that transitions near the maximum of H_{sf} should be of second order. Thus, we tend to doubt that Fig. 11(b) applies to our data. This point of view differs

from the one we expressed earlier.[5]

Figure 11(c) is a sketch of a phase diagram suggested by the data in Fig. 8. Such a phase diagram has no theoretical justification at present. It is shown here because it is consistent with the locations of all the observed anomalies in the TE and MS data. The lower portion of the line $T_c^{\perp}$ probably corresponds to pseudotransitions into a domain phase.

The AF phase may contain metastable domains. In that case it is possible that different domains undergo spin-flop transitions at slightly different magnetic fields. Such a local spin-flop transition was suggested by Wong.[35] This may explain why the spin-flop transitions (of the sample as a whole) which we observed in the MS data at $T \gtrsim 40$ K resembled second-order transitions. That is, the observed transition was an integral over a distribution of local transitions, each associated with a small discontinuity in the lattice parameters. This explanation, as well as the notion of a local spin flop, are speculative. Another recent suggestion is that the behavior in the bicritical region is due to off-diagonal terms in the spin-spin interaction.[36] Further studies of the bicritical region are necessary before a definitive interpretation can emerge.

Note added in proof. Very recently a neutron-diffraction study of this crystal was carried out at the Brookhaven National Laboratory [R. J. Birgeneau, R. A. Cowley, and H. Yoshizawa (private communication)]. The results indicate that there is no long-range order in the narrow region of the SF phase in Fig. 3 which is below 74 kOe and above the reentrant portion of the AF-SF boundary. Long-range order was observed on the SF side of the P-SF boundary when H was above about 75 kOe.

ACKNOWLEDGMENTS

We wish to thank R. J. Birgeneau, A. Aharony, P. Wong, C. C. Becerra, and A. N. Berker for useful discussions. The Francis Bitter National Magnet Laboratory is supported by the National Science Foundation through its Division of Materials Research. The Instituto de Fisica at Universidade de São Paulo is supported by Financiadora de Estudos e Projetos (FINEP). This work was supported in part by a joint grant from the U. S. National Science Foundation and the Brazilian Conselho Nacional de Desenvolvimento Científico e Technológico (CNPq).

[1]Some examples of theoretical works on the subject are Y. Imry and S.-k. Ma, Phys. Rev. Lett. **35**, 1399 (1975); G. Grinstein, *ibid.* **37**, 944 (1976); A. Aharony, Y. Imry, and S.-k. Ma, *ibid.* **37**, 1364 (1976); A. P. Young, J. Phys. C **10**, L257 (1977); A. Aharony, Phys. Rev. B **18**, 3328 (1978); E. Pytte, Y. Imry, and D. Mukamel, Phys. Rev. Lett. **46**, 1173 (1981); G. Grinstein and S.-k. Ma, *ibid.* **49**, 685 (1982).

[2]S. Fishman and A. Aharony, J. Phys. C **12**, L729 (1979).

[3]P. Wong, S. von Molnar, and P. Dimon, J. Appl. Phys. **53**, 7954 (1982); Solid State Commun. **48**, 573 (1983); P. Wong, J. W. Cable, and P. Dimon, J. Appl. Phys. **55**, 2377 (1984); P. Wong and J. W. Cable, Phys. Rev. B **28**, 5361 (1983); Solid State Commun. **51**, 545 (1984). See also J. L. Cardy, Phys. Rev. B **29**, 505 (1984).

[4]Y. Shapira, J. Appl. Phys. **53**, 1931 (1982).

[5]Y. Shapira and N. F. Oliveira, Jr., Phys. Rev. B **27**, 4336 (1983).

[6]D. P. Belanger, A. R. King, and V. Jaccarino, Phys. Rev. Lett. **48**, 1050 (1982); J. Appl. Phys. **53**, 2702 (1982).

[7]G. Grinstein, J. Appl. Phys. **55**, 2371 (1984).

[8]D. P. Belanger, A. R. King, V. Jaccarino, and J. L. Cardy, Phys. Rev. B **28**, 2522 (1983); D. P. Belanger, A. R. King, and V. Jaccarino, J. Appl. Phys. **55**, 2383 (1984); I. B. Ferreira, A. R. King, V. Jaccarino, J. Cardy, and H. J. Guggenheim, Phys. Rev. B **28**, 2522 (1983).

[9]R. J. Birgeneau, H. Yoshizawa, R. A. Cowley, G. Shirane, and H. Ikeda, Phys. Rev. B **28**, 1438 (1983). See also M. Hagen, R. A. Cowley, S. K. Satija, H. Yoshizawa, G. Shirane, R. J. Birgeneau, and H. J. Guggenheim, *ibid.* **28**, 2602 (1983).

[10]R. A. Cowley, R. J. Birgeneau, G. Shirane, and H. Yoshizawa, in *Multicritical Phenomena,* edited by R. Pynn and A. Skjeltorp (Plenum, New York, 1984); R. J. Birgeneau, R. A. Cowley, G. Shirane, and H. Yoshizawa, J. Stat. Phys. **34**, 817 (1984); R. J. Birgeneau (private communication).

[11]J. Villain, Phys. Rev. Lett. **23**, 1543 (1984). See also R. Bruinsma and G. Aeppli, *ibid.* **23**, 1547 (1984).

[12]R. A. Cowley and W. J. L. Buyers, J. Phys. C **15**, L1209 (1982).

[13]Northern Analytical Laboratory, Amherst, NH, and Analytical Laboratory, Center for Materials Science and Engineering, MIT.

[14]H. H. Sample, B. L. Brandt, and L. G. Rubin, Rev. Sci. Instrum. **53**, 1129 (1982). These results were confirmed by our own measurements in the range $37 < T < 45$ K and $0 < H \leq 80$ kOe.

[15]The transition in Fig. 2 is slightly wider than in Fig. 1, presumably because the field alignment is less accurate. [See I. S. Jacobs, J. Appl. Phys. **32**, Suppl. 61 (1961)].

[16]L. J. de Jongh and A. R. Miedema, Adv. Phys. **23**, 1 (1974).

[17]A. Brooks Harris and S. Kirkpatrick, Phys. Rev. B **16**, 542 (1977).

[18]C. Trapp and J. W. Stout, Phys. Rev. Lett. **10**, 157 (1963).

[19]S. Foner, in *Magnetism,* edited by G. T. Rado and H. Suhl (Academic, New York, 1963), Vol. I, pp. 383 ff.

[20]U. Gäfvert, L. Lundgren, P. Nordblad, B. Westerstrandh, and O. Beckman, Solid State Commun. **23**, 9 (1977).

[21]Y. Shapira and J. Zak, Phys. Rev. **170**, 503 (1968); R. L. Melcher, Phys. Rev. Lett. **25**, 1201 (1970).

[22]S. M. Rezende, A. R. King, R. M. White, and J. P. Timbie, Phys. Rev. B **16**, 1126 (1977); **16**, 5130(E) (1977).

[23]Y. Shapira and S. Foner, Phys. Rev. B **1**, 3083 (1970); Y. Shapira and C. C. Becerra, Phys. Lett. **57A**, 483 (1976); **58A**, 493 (E) (1976).

[24]F. G. Brady Moreira, I. P. Fittipaldi, S. M. Rezende, R. A. Tahir-Kheli, and B. Zeks, Phys. Status Solidi B **80**, 385 (1977).

[25]F. G. Brady Moreira and I. P. Fittipaldi, J. Appl. Phys. **50**, 1726 (1979); S. Foner, in *Proceedings of the International*

Conference on Magnetism, Nottingham, 1964 (Institute of Physics and Physical Society, London, 1964), p. 438; M. C. K. Wiltshire, J. Phys. C **10**, L37 (1977); W. E. Tennant and P. L. Richards, *ibid.* **10**, L365 (1977); G. J. Coombs, R. A. Cowley, W. J. L. Buyers, E. C. Svensson, T. M. Holden, and D. A. Jones *ibid.* **9**, 2167 (1976); W. J. L. Buyers, D. E. Pepper, and R. J. Elliott, *ibid.* **6**, 1933 (1973); A. R. King, S. M. Rezende, and V. Jaccarino. Bull. Am. Phys. Soc. **22**, 332 (1977).

[26]S. Galam and A. Aharony, J. Phys. C **13**, 1065 (1980).

[27]A. B. Pippard, *Elements of Classical Thermodynamics* (Cambridge University Press, London, 1966).

[28]R. J. Birgeneau, R. A. Cowley, and H. Yoshizawa (private communication).

[29]K. E. Newman and E. K. Riedel, Phys. Rev. B **25**, 264 (1982).

[30]G. Jug, Phys. Rev. B **27**, 609 (1983).

[31]H. Rohrer, J. Appl. Phys. **52**, 1708 (1981).

[32]M. E. Fisher, Phys. Rev. Lett. **34**, 1634 (1975).

[33]A. R. King and H. Rohrer, Phys. Rev. B **19**, 5864 (1979).

[34]A. Aharony, Ref. 1 (1978 paper).

[35]P. Wong (private communication).

[36]P. Wong and J. W. Cable, Phys. Rev. B **30**, 485 (1984).